

Manuscript version: Author's Accepted Manuscript

The version presented in WRAP is the author's accepted manuscript and may differ from the published version or Version of Record.

Persistent WRAP URL:

<http://wrap.warwick.ac.uk/147758>

How to cite:

Please refer to published version for the most recent bibliographic citation information. If a published version is known of, the repository item page linked to above, will contain details on accessing it.

Copyright and reuse:

The Warwick Research Archive Portal (WRAP) makes this work by researchers of the University of Warwick available open access under the following conditions.

Copyright © and all moral rights to the version of the paper presented here belong to the individual author(s) and/or other copyright owners. To the extent reasonable and practicable the material made available in WRAP has been checked for eligibility before being made available.

Copies of full items can be used for personal research or study, educational, or not-for-profit purposes without prior permission or charge. Provided that the authors, title and full bibliographic details are credited, a hyperlink and/or URL is given for the original metadata page and the content is not changed in any way.

Publisher's statement:

Please refer to the repository item page, publisher's statement section, for further information.

For more information, please contact the WRAP Team at: wrap@warwick.ac.uk.

Adaptive and optimum secret key establishment for vehicular communications and sensing

Abstract—Confidentiality is a major concern in any wireless communication, especially so in vehicular networks where cyber-attacks easily evolve in the loss of human lives or assets. In these scenarios, the current proposed approach relies on public-key cryptography which, however, requires significant computational capabilities for the encryption/decryption process and large bandwidth for keys distribution. To overcome these limitations, physical-layer security has been proposed to provide confidentiality by exploiting the physical characteristics of the wireless medium. Nonetheless, the high dynamicity and heterogeneity of vehicular environments require the design of secure protocols that are able to self-configure and adapt to all conditions, free from any fixed choice of parameters. In this paper, we propose a secure scheme composed by a novel quantisation approach in which thresholds are analytically derived from the statistics of the channel, mathematically guaranteeing the robustness of the protocol. Moreover, we design an optimisation engine to continuously adapt the system to run in its optimal conditions. The performance of the proposed scheme is evaluated through extensive simulation in order to demonstrate its significant improvement to the existing approach.

Index Terms—Physical layer security, Lossy quantisation, VANETs, Channel Reciprocity Adaptation, RSS

I. INTRODUCTION

Wireless communication technologies provide the essential scalability required by the continuous increase of interconnected devices. In the case of Intelligent Transport Systems (ITS), electrical engineering together with computer science as well as, transport engineering and communication networks synergistically collaborate to improve transport safety and quality. ITS services span across different areas, as in the Advanced Traveller Information System, which provides drivers with real-time route information and the Advanced Transportation Management System that coordinates traffic control devices. Nonetheless, the most anticipated ITS applications arise from vehicle-infrastructure and vehicle-vehicle integrations. These applications rely on the collaboration between vehicles and road infrastructure and hence becomes the key factor in reducing the risk of accidents and environmental impact. A typical vehicle ad-hoc network (VANET) includes on-board units (OBUs) and road-side units (RSUs) which communicate through dedicated short-range communication (DSRC). Security is the first priority [1], [2] as the wireless medium opens up the possibility for unauthorised users to passively eavesdrop and/or to alter the transmissions [3]. Data confidentiality is traditionally provided by cryptographic mechanisms implemented in upper layers of the Open System Interconnection (OSI) model. Encryption approaches can be

classified in two categories: symmetric (secret key) and asymmetric (public key) solutions [4].

The present security proposal is based on public-key infrastructure (PKI) to provide authentication, confidentiality, identity and non-repudiation. PKI cryptographic primitives are computationally complex and OBUs may still need hundreds of milliseconds to complete such operations, responsible for unacceptable delays when transmitting safety-related messages [5]. Furthermore, PKI is intrinsically a centralised approach where a trusted authority distributes and manages keys and certificates however, its adaptation to highly distributed and ad-hoc network rises scalability challenges [6]. On the other hand, symmetric cryptography is more power/computational efficient than PKI but its applications are drastically limited by the delicate tasks of distributing and storing the secret keys. Distribution usually requires a secondary secure channel which is hardly feasible, especially in VANETs due to their highly dynamic topology.

In these challenging scenarios, Physical Layer Security (PLS) has emerged as a technique to provide unconditionally secure communications by efficiently exploiting the wireless medium [7] as a shared source of randomness to extract symmetric keys. Randomness is a consequence of the unpredictability of the multipath phenomena [8], where the received wireless signal is altered by the superposition of different transmitted echoes, coming from different paths with different phases. Keys are generated through the quantisation of channel properties, which are considered stochastic processes, such as the Received Signal Strength (RSS) or the phase [9]. Keys distribution is avoided by channel reciprocity principle, which states that in sufficiently small-time intervals, referred to as coherence intervals, the Channel Impulse Response (CIR) is substantially constant [10]. This way, the communicating parties can probe the channel in an interleaved fashion, obtaining similar estimates inside the same intervals and therefore, generating the same keys. Nonetheless, estimates gathered by third entities are statistically uncorrelated due to spatial and time variability of multipath phenomena, leading to different useless keys and providing confidentiality to the communication.

In the PLS process, quantisation plays a crucial role since its performance greatly affects the overall system efficiency and robustness. Quantisation not only does it transform an analogous physical quantity in a stream of discrete numbers, but it also reduces differences among estimates taken by the legitimate parties, even in the same coherence interval. These variations are caused by hardware differences, asymmetric noise and mainly, by the half-duplex nature of wireless de-

vices, unable to receive and transmit at the same time [11]. All these effects are included in the term imperfect reciprocity. Even a single different bit makes the generated keys unusable, nullifying all efforts in the extraction process.

Another aspect to be taken into account is the entropy (H) of the extracted sequences, which measures their level of randomness [12]. The latter is a crucial property of cryptographic keys to remove possible statistical defects that could ease the attacks conducted by adversaries with active or passive presence to the channel [13].

What makes the design of PLS-protocols challenging, is the conflicting relationship among the throughput of the quantisation (bit-generation rate or BGR), the inevitable presence of erroneous bits (bit-mismatch rate or BMR) and the entropy of the resulting streams. In their attempt to optimise the corresponding proposed schemes, most literature sources address only a subset of the metrics introduced above, coming up with resulting in sub-optimal results [9].

Only few protocols in literature take the imperfect reciprocity into account [14], [15], [16] considered as a constant aspect of the environment. In other the studies [17], [18] non-reciprocity is simply ignored during quantisation and fully tackled in the error correction stage. Furthermore, to the best of our knowledge, there isn't a scheme which considers a continuously varying reciprocity due to changing environmental conditions and dynamic network topology. To fill these gaps, to the best of our knowledge, for the first time in the existing literature:

- 1) We prove the existence of optimal thresholding strategies within a two-level RSS-based quantisation block, which strike an optimal balance among the evaluation metrics (BGR, BMR and H). Moreover, thresholds are not fixed system parameters but continuously derived by the channel's statistics. Specifically, we introduce the use of the Cumulative Distribution Function (CDF) and Average Fade Duration (AFD) to mathematically create equiprobable regions. This way, our scheme outperforms the classical implementation proposed in [19], providing the minimum BMR, the maximum BGR and the maximum key entropy H .
- 2) We address the continuously varying reciprocity of the channel with the introduction of a novel Perturb & Observe algorithm. In a two-steps approach, we first unify BMR and BGR under a criterion named as secret-bit generation rate (SBGR) that accounts for the number of correct bits per channel sample hence, representing an efficient comparator for different quantisation schemes. Secondly, we design and develop the algorithm acting as a feedback in the key-extraction process. This algorithm is self-configurable and able to adapt to sharp changes in the channel and reciprocity parameters, while continuously observing the SBGR performance to adjust quantisation thresholds accordingly.

The remaining part of this paper is organised as follows: Section II reviews existing studies on PLS in vehicle-to-vehicle communication, focusing on RSS quantisation schemes. Sec-

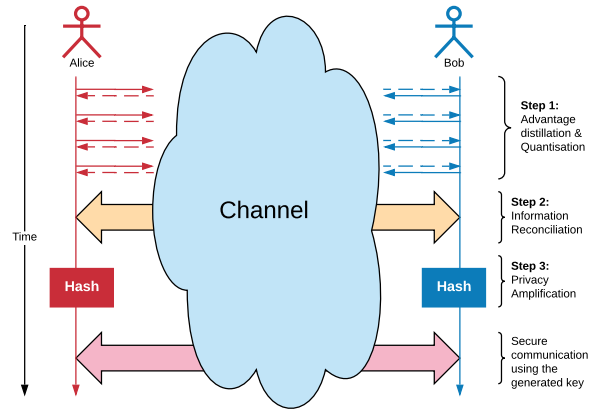


Fig. 1. PLS Key extraction process: Alice and Bob exchange probes in order to agree on a key.

tion III introduces the V2V channel model and the quantisation performance metrics; Section IV explains the novel techniques of analytical thresholding, introducing and underlying the proposed optimisation algorithm. Section V compares and contrasts the simulations' results with the standard level-crossing method (hereinafter referred to as STD) [19]. Finally, Section VI draws the conclusions of the present piece of research.

II. RELATED WORKS

The research branch on PLS started with Wyner [20] who showed how it is possible to establish secure transmissions in scenarios where the eavesdropper (Eve) has a lower quality channel available than the communicating nodes (Alice and Bob). This difference of links' quality translates into a difference of channel capacities, referred to as secrecy capacity, which can be exploited to send private information. Maurer [21] and Ahlswede-Csiszar [22] demonstrated that confidentiality is also achievable when the attacker observes a higher quality link than the one available to authorised parties. Their technique is based on the extraction of a secret key over the public and insecure channel.

The key extraction process is shown in figure 1 and composed by three fundamental steps: advantage-distillation, information reconciliation and privacy amplification. In the first phase, legitimate parties probe the channel, in order to acquire a number of estimates proportional to the desired key-length. To collect correlated measurements, Alice and Bob must sense the medium inside the same coherence time, defined as the time period over which the channel impulse response is considered constant. Coherence time depends on the Doppler effects due to nodes mobility [8]. Extracted estimates are then converted into bit-streams through quantisation and sent to the information reconciliation phase. The latter has the duty to fix any bit disagreements with the aid of error correcting codes and public discussion through the insecure channel. A widely used technique is CASCADE [23] in which parties randomly

188 permute the sequences and recursively exchange parity check
 189 information. More sophisticated schemes are based on turbo
 190 codes [17] and low-density parity check (LDPC) [24] which
 191 both try to maximise reconciliation capabilities as well as,
 192 simultaneously minimise the leakage of information to the
 193 eavesdropper. Alice and Bob's sequences should now be
 194 identical, otherwise the entire extraction process is restarted.
 195 However, to use such strings as keys, the last step of privacy
 196 amplification strengthens them by improving their entropy, as
 197 for example with the application of universal hash functions
 198 and/or one-way functions [25].

199 This investigation focuses on the RSS quantisation for
 200 its ease of use and the immediate availability in all out-
 201 of-the-shelf wireless devices [26]. Furthermore, RSS greatly
 202 benefits from nodes' mobility, the main property of VANETs,
 203 generating keys at a fast rate and with high entropy. In their
 204 pioneer study [27], Tope et al. analysed the signal attenuation
 205 by collecting estimates of the envelope of received packets
 206 and storing them into arrays. By subtracting half of the
 207 latter from the other half, the scheme removed the path-
 208 loss contribution, which is correlated to distance and hence
 209 predictable. Two thresholds were used to drop estimates that
 210 have a high probability of being either foreseeable or converted
 211 to mismatching bits. Azimi-Sadjadi et al. [28] proposed the
 212 use of deep fades or local minima of the signal to improve
 213 keys agreement. Deep fades were detected by first quantising
 214 RSS estimates, using a single threshold and then by searching
 215 for runs of 1-bits of sufficient length. At this point, Alice
 216 can transmit the hash of the generated key to Bob, who
 217 compensates any disagreements by exploring a small search-
 218 space due to deep fades' statistical properties. Inspired by
 219 the previous idea, Mathur et al. [19] introduced a quantiser
 220 with two thresholds, whose distance is proportional to the
 221 standard deviation of an array of estimates. The quantisation
 222 bin between thresholds is referred to as censor or invalid
 223 region, where values are dropped because of their high proba-
 224 bility of disagreement. Furthermore, only the estimates located
 225 inside sequences of sufficient excursions above or below the
 226 thresholds are considered to discard sharp changes in the signal
 227 amplitude. This constraint has been relaxed in a few derived
 228 works [17], [29], [30], where the increased error probability
 229 was counterbalanced by a more efficient reconciliation tech-
 230 nique. Instead of using absolute thresholds, the research [31]
 231 proposed a differential approach where quantisation operates
 232 on the difference between two consecutive RSS values. This
 233 way, the scheme is able to provide better results, while being
 234 resistant to RSS-manipulation attacks. Since increasing the
 235 number of quantisation levels could have a negative impact on
 236 BMR, the study [32] introduced the use of vector quantisation
 237 to increase BGR. In the latter, RSS estimates are reused n
 238 times, where n is the dimension of the vector. While this
 239 approach could achieve better BGR without increasing BMR,
 240 it remains to investigate the security aspects related to the es-
 241 timates' recycling. VANETs communication constraints have
 242 been considered in [33], where the authors designed a key-
 243 length optimisation algorithm. Starting from the characteristics

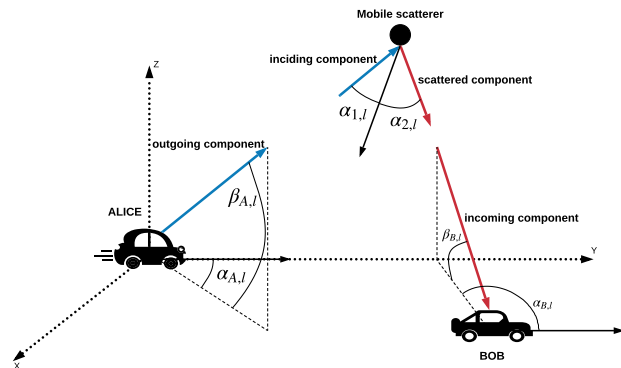


Fig. 2. V2V channel model: two vehicles are moving in a three-dimensional environment including mobile scatterers.

244 of the specific scenario, such as the location of the parties and
 245 an estimate of the coherence time, the algorithm attempts to
 246 extract a key with as much robustness as possible.

247 Only few protocols in literature take the imperfect reci-
 248 procity into account. Half-duplex limitations are addressed
 249 in [14], [15] by applying fractional interpolation in order
 250 to virtually measure estimates at the same time instants.
 251 Moreover, non-reciprocity due to hardware differences are
 252 removed with a ranking method in [16]. In [34] noise is
 253 reduced by smoothing the readings, using sliding windows
 254 whose weights are collaboratively generated by Alice and Bob.

255 III. CHANNEL MODEL AND PERFORMANCE METRICS

256 The high dynamicity of VANETs constantly changes the
 257 physical characteristics of the wireless media. In fact, the mul-
 258 tipath phenomena induce a time-variant impulse response, the
 259 receiver to collect a train of echoes of the transmitted message,
 260 which travels different paths and arrives at the destination
 261 with different delays and attenuation factors [8]. Just as the
 262 mobility of vehicles and intermediate objects appear to be un-
 263 predictable, so are the multipath effects on the received signals.
 264 In deterministic channel models, the propagation environment
 265 is recreated through ray-tracing techniques [35]. Nonetheless,
 266 a detailed description of both objects' specific coordinates and
 267 electrical characteristics is crucial to achieve accurate results,
 268 rendering this approach hardly generalisable to all possible
 269 operating conditions. On the other hand, stochastic models
 270 consider the wireless medium as a random process, whose
 271 statistics provide an inner sight of the channel properties [36].
 272 Moreover, random approaches provide numerical stability and
 273 combine high performances and ease of implementation. For
 274 these reasons, in the current investigation we opted to use a
 275 generic stochastic model [37], which proved to be a complete,
 276 configurable and tuneable model for key-generation.

277 A. V2V generic stochastic model

278 Figure 2 shows the considered three-dimensional V2V sce-
 279 nario, where propagation's parameters and entities' locations
 280 are driven by a Monte Carlo process [38], [39]. Two vehicles,

281 Alice and Bob, are equipped with a single antenna and move
 282 at speeds $u_{A(B)}$. Alice's signals are received by Bob as the
 283 superposition of a number L of different echoes, unresolvable
 284 in delay. Each l -th multipath component reaches its destination
 285 with a specific complex amplitude a_l and phase ϕ_l caused by
 286 the different path it has travelled. To adequately approximate
 287 a trafficked urban scenario, we also considered the interaction
 288 with mobile scatterers moving at speed u_S [37].

289 In this environment, Alice's channel estimates G_A are
 290 generated by the following formula [37]:

$$G_A(t) = \sum_{l=1}^L |a_l| \exp(j\phi_l) \exp(j2\pi v_l t) \quad (1)$$

291 where t is the time and v_l the Doppler shift of the l -th
 292 multipath component. The latter is the sum of the contributions
 293 of the transmitter $v_{A,l}$, receiver $v_{B,l}$ and scatterers $v_{S,l}$, as
 294 follows:

$$v_l = v_{A,l} + v_{B,l} + v_{S,l} \quad (2)$$

$$v_{A(B),l} = v_{A(B)_{max}} \cos \alpha_{A(B),l} \cos \beta_{A(B),l} \quad (3)$$

$$v_{S,l} = v_{S_{Wb}} (\cos \alpha_{1,l} + \cos \alpha_{2,l}) \quad (4)$$

297 In the previous equations, $\alpha_{A(B),l}$ and $\beta_{A(B),l}$ are azimuth
 298 and elevation angles of departure (arrival) and $\alpha_{1,l}, \alpha_{2,l}$ cor-
 299 respond to the incoming and outgoing components at the
 300 mobile scatterer. Maximum Doppler shifts $v_{A(B)_{max}}$ arise
 301 from nodes' mobility, hence

$$v_{A(B)_{max}} = \frac{u_{A(B)_{max}}}{\lambda} = u_{A(B)_{max}} \cdot f_c / c \quad (5)$$

$$v_{S_{Wb}} = \frac{u_{S_{Wb}}}{\lambda} = u_{S_{Wb}} \cdot f_c / c \quad (6)$$

303 where $u_{A(B)_{max}}$ are the corresponding maximum velocities,
 304 λ is the carrier's wavelength at frequency f_c and c is the speed
 305 of light. The speed of mobile scatterers $v_{S_{Wb}}$ is randomised
 306 through a Weibull distribution, in order to adequately associate
 307 most multipath power contribution to static and slowly moving
 308 objects [37] thus,

$$p_{u_S}(u_{S_{Wb}}) = w_{Wb} u_{S_{Wb}}^{a_{Wb}-1} \exp(-w_{Wb} u_{S_{Wb}}^{a_{Wb}} / a_{Wb}) \quad (7)$$

309 having scale w_{Wb} and shape a_{Wb} . Once we have Alice's
 310 estimates we need to properly generate the corresponding
 311 Bob's values in order to realistically simulate the effects of
 312 imperfect reciprocity. This loss of correlation is the direct
 313 consequence of slightly different channel state information
 314 (CSI) sensed by legitimate parties. According to the study [40],
 315 that difference is composed by a stable component and a noisy
 316 part, which are estimated after a non-reciprocity learning phase
 317 of M probes extracted from the same coherence intervals thus,

$$\mu_t = \frac{1}{M} \sum_{i=1}^M (G_{A,i}(t) - G_{B,i}(t)) \quad (8)$$

$$\sigma_C^2 = \frac{1}{M} \sum_{i=1}^M (G_{A,i}(t) - G_{B,i}(t) - \mu_t)^2 \quad (9)$$

318 The stable portion μ_t is removed by the Channel Gain Com-
 319 plement (CGC) method, leaving only the noisy component
 320 which is assumed to follow a zero-mean Gaussian distribution,
 321 thus $N(0, \sigma_C^2)$. Bob's values can now be obtained adding a
 322 normal random variable to Alice's estimates as follows: [40]:

$$G_B(t) = G_A(t) + N(0, \sigma_C^2) \quad (10)$$

323 The impact of the noisy component usually depends on
 324 the environmental conditions, which are dynamic and unpre-
 325 dictable, especially in VANETs. In this respect, our proposed
 326 algorithm aims to rapidly adapt quantisation thresholds to
 327 the available amount of channel reciprocity, modelled as a
 328 continuously changing standard deviation σ_C .

B. Key performance metrics 329

330 In order to compare the proposed algorithm to the other
 331 schemes in literature, it is necessary to introduce the perfor-
 332 mance metrics [41]. The quantisation performance is measured
 333 by the bit generation rate (BGR), which is the average number
 334 of bits that can be extracted per channel estimate or per unit
 335 time. The former definition is preferable, as it does not depend
 336 on the chosen probing rate. Thus

$$BGR = \frac{no.extracted\ bits}{no.channel\ samples} \quad (11)$$

337 Higher value of BGR indicates a faster production of bit-
 338 streams which, in turn, translates to keys being generated in
 339 less time and hence refreshed continuously.

340 Another relevant performance criterion is the bit-mismatch
 341 rate (BMR) defined as the ratio of the number of erroneous
 342 bits (i.e. they don't match between Alice and Bob) to the total
 343 amount of extracted bits

$$BMR = \frac{no.erroneous\ bits}{no.channel\ samples} \quad (12)$$

344 BMR determines the system resilience against noise and
 345 interferences, defined after the quantisation stage or after the
 346 information reconciliation. In the first case, BMR depends only
 347 on how the quantisation space is configured (as for example
 348 the number of thresholds). On the other hand, if BMR is
 349 defined after information reconciliation, it will also embrace
 350 the error-correcting capabilities of the protocol, having the
 351 unrecoverable bits at the numerator. As our thresholding
 352 optimisation engine aims to increase the number of valid keys,
 353 it is reasonable to define BMR after reconciliation, taking
 354 advantage of any implementation of the latter.

355 Considering that the extracted sequences will be treated
 356 as cryptographic keys, it is important they possess enough
 357 entropy, ideally close to 1, to maximise the uncertainty from
 358 an attacker's point of view. Entropy of bit i is measured by
 359 the following formula [17]:

$$H_i = -p_{0,i} \log p_{0,i} - (1 - p_{0,i}) \log(1 - p_{0,i}) \quad (13)$$

where $p_{0,i}$ is the posterior probability of bit i being 0. The maximum value of 1 indicates equal probability of having bits 1 or 0, i.e. $p_0 = 1 - p_0 = 0.5$. For independent bit-strings of length N , the total entropy is defined as $H_{total} = (\sum_{i=1}^N H_i)/N$. Entropy alone is not sufficient to prove the absence of statistical defects in the bit sequences. For example, they may contain long runs of the same bit and the repetition of sub-parts. For these reasons, in all our tests we also evaluate key robustness against the random-tests suite, provided by the National Institute of Standards and Technology (NIST) [13].

IV. ANALYTICAL QUANTISATION THRESHOLDING

Our secret-key extraction algorithm follows from work introduced in [19], where legitimate nodes locally convert their RSS-estimates in bit-streams, prior to symmetric key generation. Channel probing is done in half-duplex mode, hence Alice and Bob extract samples from the same coherence intervals in an interleaved fashion. The inability to probe at the same time instants introduces a small, yet unpredictable variation in the channel response. The latter, together with other environmental factors, reduce the channel reciprocity as well as, increase the probability of extracting different key-candidates thus, they reduce the effectiveness of the extraction process. In order to reduce BMR, we apply a two-level ‘‘censor’’ quantisation function defined as follows:

$$Q(x) = \begin{cases} 1, & \text{if } x > q_+ \\ 0, & \text{if } x < q_- \\ \text{dropped} & \text{otherwise} \end{cases} \quad (14)$$

Estimates in the interval $q_- \leq x \leq q_+$ are dropped in accordance with their higher probability of being translated into different bits at both communication ends. On the other hand, the censor region has a direct impact of the throughput of the quantisation stage and its size should be set as the optimal trade-off between BMR and BGR metrics. In STD thresholds were originally computed using average and standard deviation of an array of samples \underline{h} , thus

$$q_{\pm} = \text{average}(\underline{h}) \pm \alpha_{STD} \cdot \text{stdev}(\underline{h}) \quad (15)$$

where parameter α_{STD} expresses the relationship between the censor region and how spread out the values are and is set empirically. To compare STD with our proposed methods we define a novel metric, namely the secret-bit generation rate (SBGR), as the ratio of the number of bits which are successfully used to compose keys to the total amount of channel samples that were used, thus

$$SBGR = \frac{\text{no.keybits}}{\text{no.channel samples}} \quad (16)$$

Remembering that BMR is defined after information reconciliation, the number of keybits corresponds to the amount of

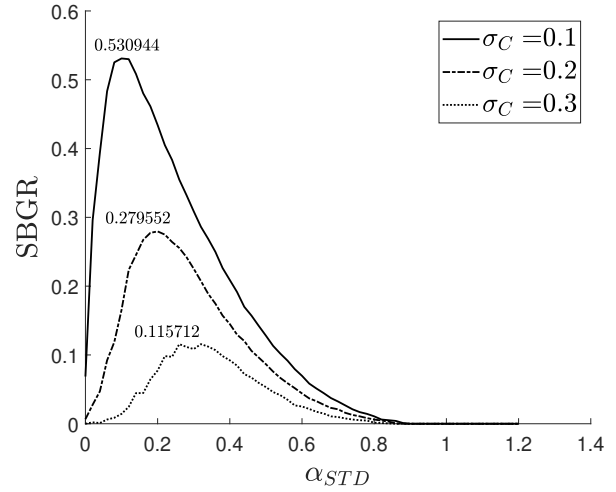


Fig. 3. SBGR against α_{STD} for different non-reciprocity factors in the standard censor approach.

successfully generated bits after errors correction, which can be expressed as

$$\text{no.keybits} \leq \text{no.samples} \cdot BGR \cdot (1 - BMR) \quad (17)$$

where the less-than-equal symbol arises from the fact that a single erroneous bit eventually compromises an entire key. By merging equations 16 and 17

$$SBGR \leq BGR \cdot (1 - BMR) \quad (18)$$

Equation 18 elicits how the new metric embraces both the effects of BGR and BMR. Moreover, SBGR is evaluated after errors correction, making the optimisation engine capable of taking advantage of any existing or future reconciliation schemes. Figure 3 shows SBGR against different invalid region sizes modelled through the parameter α_{STD} in e.q. 15 and for different non-reciprocity settings, represented by standard deviation σ_C in e.q. 9. SBGR performance increases as channel non-reciprocity (σ_C) reduces. Simulation parameters are shown in table I.

Given the fact that all curves express a single (global) maximum, a Hill-climbing algorithm seems to be a simple, yet effective approach to locate the point with highest performance. The idea is to ‘modulate’ the quantisation thresholds, according to the resulting SBGR, in an attempt to identify the optimal set-point. However, as stated in the introduction, a high entropy H of the generated bit-streams is a mandatory requirement to guarantee the statistical robustness of the resulting symmetric keys. As this aspect is not covered by the definition of SBGR, we decided to mathematically relate the thresholds to ensure the maximum entropy.

A. CDF-based thresholding strategy

The first proposed strategy is based on the cumulative distribution function (CDF) $F_X(\cdot)$. In the case of two-level

430 quantisation, optimal key-entropy is guaranteed by forcing
 431 thresholds q_{\pm} to generate equiprobable regions, thus

$$F_X(q_-) = Pr(-\infty < x \leq q_-) \\ = Pr(q_+ \leq x < +\infty) = 1 - F_X(q_+) \quad (19)$$

432 In the absence of a significant line-of-sight (LOS) com-
 433 ponent, Rayleigh distribution has proved to model channel
 434 propagation adequately [37]. Rayleigh's CDF is defined as
 435 follows:

$$F_X(x) = 1 - \exp\left(-\frac{x^2}{2\sigma^2}\right) \quad (20)$$

436 By merging 19-20

$$F_X(q_-) = 1 - \exp\left(-\frac{q_-^2}{2\sigma^2}\right) \\ = \exp\left(-\frac{q_+^2}{2\sigma^2}\right) = 1 - F_X(q_+) \quad (21)$$

437 where upper threshold q_+ can be derived by applying the
 438 logarithm to the reciprocal of the first side (due to the minus
 439 sign inside the second exponential) and extracting the square
 440 root, thus

$$q_+ = \sqrt{2}\sigma \sqrt{\log\left(\frac{1}{1 - \exp\left(-\frac{q_-^2}{2\sigma^2}\right)}\right)} \quad (22)$$

441 B. ADF-based thresholding strategy

442 The second proposed method is based on the use of average
 443 fade duration (AFD), a second-order statistical parameter,
 444 which should better capture channel variabilities and simul-
 445 taneously maintain a sufficient level of key robustness. AFD
 446 is defined as

$$T(z) = F_X(z)/N(z) \quad (23)$$

447 that is, the ratio between the cumulative distribution function
 448 $F_X(\cdot)$ and the level crossing rate (LCR) $N(\cdot)$. In Rayleigh
 449 environments LCR is expressed by the following formula [37]

$$N(z) = \sqrt{\frac{d_1}{2\pi}} \exp\left(-\frac{z^2}{2\sigma^2}\right) \frac{z}{\sigma^2} \quad (24)$$

450 where parameter d_1 depends on vehicles' speeds and multi-
 451 path angular spread (see [37] for details). The core concept
 452 in this method is to ensure that when a signal crosses a
 453 threshold, it will remain in the corresponding region for the
 454 same (averaged) time duration. Mathematically,

$$T(q_-) = T^c(q_+) \quad (25)$$

455 where $T^c(z) = (1 - F_X(z))/N(z)$ is also commonly
 456 referred to as connection time. By merging equations 20, 23
 457 and 25

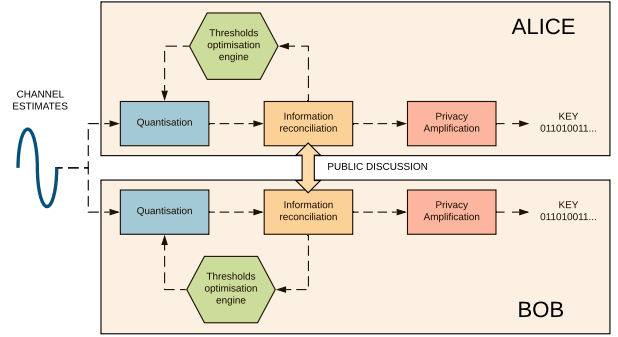


Fig. 4. Thresholds optimisation engine acts as a feedback in PLS key-generation process.

$$T(q_-) = \frac{1 - \exp\left(-\frac{q_-^2}{2\sigma^2}\right)}{\sqrt{\frac{d_1}{2\pi}} \exp\left(-\frac{q_-^2}{2\sigma^2}\right) \frac{q_-}{\sigma^2}} \\ = \frac{\exp\left(-\frac{q_+^2}{2\sigma^2}\right)}{\sqrt{\frac{d_1}{2\pi}} \exp\left(-\frac{q_+^2}{2\sigma^2}\right) \frac{q_+}{\sigma^2}} = T^c(q_+) \quad (26)$$

458 which, in turns, simplifies to

$$\frac{1 - \exp\left(-\frac{q_-^2}{2\sigma^2}\right)}{\exp\left(-\frac{q_-^2}{2\sigma^2}\right) q_-} = \frac{1}{q_+} \quad (27)$$

459 Once again, the upper threshold q_+ can be derived from the
 460 lower one q_- as follows:

$$q_+ = \frac{q_-}{\exp\left(-\frac{q_-^2}{2\sigma^2}\right) - 1} \quad (28)$$

461 Whenever it is needed to adapt the quantisation thresholds,
 462 the two proposed strategies provide an analytic way to derive
 463 the invalid region's boundaries, enforcing maximum entropy
 464 as well as, preparing the ground for the upcoming SBGR
 465 optimisation block.

466 C. Thresholds Optimisation engine

467 In this section we introduce an optimisation algorithm
 468 in the standard process of key extraction to recognise the
 469 maximum SBGR performance of the system without relying
 470 on the choice of fixed quantisation parameters. Figure 4
 471 shows that the novel block acts as feedback from the stage
 472 information reconciliation to adapt the quantisation parameters
 473 by continuously monitoring the output of the key-extraction
 474 process. Inside this block, a Perturb & Observe (PO) algorithm
 475 constantly alters the invalid region size and monitors the
 476 effects on the resulting SBGR. In doing so, PO can adapt to
 477 different scenarios, even within the ones with variable channel
 478 reciprocity, a common condition holding in VANETs. For the
 479 sake of simplicity, the algorithm perturbs the size of the censor
 480 region by a positive amount $\delta > 0$, acting on the lower

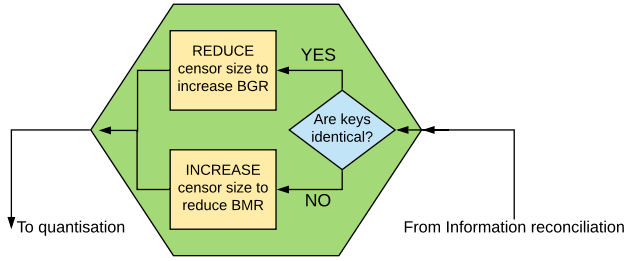


Fig. 5. A simplified view of the optimisation block: reconciliation outcome is used to adapt thresholds distance.

481 threshold q_- and leaving the corresponding upper threshold
 482 q_+ computed accordingly to the chosen strategy (CDF-based
 483 or AFD-based). Figure 5 shows the intuitive underlying idea:
 484 if the generated bitstreams are different after reconciliation,
 485 this indicates a decrease in channel reciprocity, which should
 486 be balanced by a larger censor region. On the other hand,
 487 matching keys suggest the possibility to reduce thresholds'
 488 distance further, thus, aiming for higher BGR.

489 The frequency with which the system should be perturbed
 490 must be carefully chosen: if thresholds are modulated too
 491 often, they can generate a significant oscillation around the
 492 optimal SBGR, preventing complete convergence. On the other
 493 hand, if the algorithm does not calibrate itself fast enough, it
 494 may not be able to reach optimality before the medium has
 495 moved to a different reciprocity condition. To strike a balance,
 496 it seems reasonable to perturb quantisation bins after a mini-
 497 mum number of events. More specifically, the algorithm waits
 498 for a number $INT_{SUCCESS}$ of successful keys before reduc-
 499 ing the censor size and a number of INT_{FAIL} failed attempts
 500 before increasing it. Usually $INT_{FAIL} \leq INT_{SUCCESS}$
 501 because it is safer to faster adapt to worse conditions than
 502 to improve already good ones.

503 Another improvement stems from the consideration that
 504 when the algorithm has successfully reached the optimal
 505 point, even the smallest positive and negative perturbation
 506 would possibly result in a waste of bits or the total rejection
 507 of the generated bitstreams. For that reason, the algorithm
 508 simultaneously quantifies the channel estimates against three
 509 pairs of thresholds $q_{\pm}^{(1)}, q_{\pm}^{(2)}, q_{\pm}^{(3)}$ whose lower parts are spaced
 510 by $\delta > 0$, thus

$$q_-^{(1)} = q_-^{(2)} + \delta \quad (29)$$

$$q_-^{(3)} = q_-^{(2)} - \delta \quad (30)$$

512 Considering that the formulae 22 and 28 are decreasing
 513 monotonic functions, the three regions are in the following
 514 order relation

$$(q_+^{(1)} - q_-^{(1)}) \leq (q_+^{(2)} - q_-^{(2)}) \leq (q_+^{(3)} - q_-^{(3)}) \quad (31)$$

515 Recalling that smaller regions generate higher BGR as well
 516 as higher BMR, we will refer to those pairs hereafter as ag-

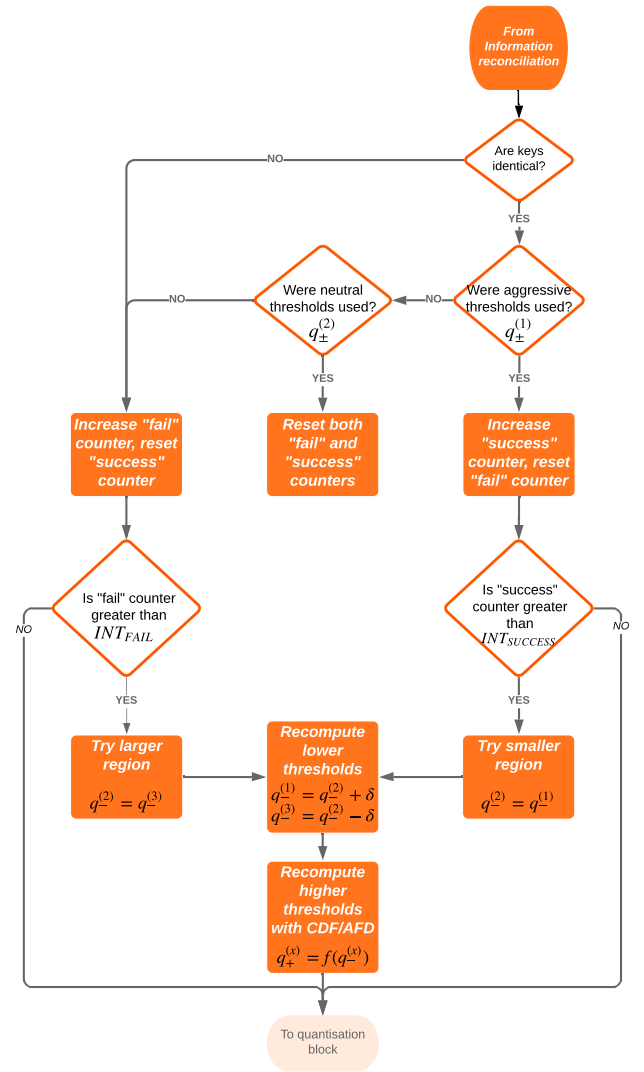


Fig. 6. Flowchart of PO algorithm where quantisation thresholds are adjusted to achieve the maximum key-generation rate.

517 aggressive thresholds $q_{\pm}^{(1)}$, neutral thresholds $q_{\pm}^{(2)}$ and defensive
 518 thresholds $q_{\pm}^{(3)}$ which will be further evaluated in this specific
 519 order.

520 Figure 6 shows the complete algorithm flowchart, which can
 521 be best explained by considering three possible conditions:
 522 firstly, the algorithm is using a censor region's size which is
 523 larger than the optimal one for the current reciprocity factor,
 524 dropping estimates that can be safely transformed into keybits.
 525 In that case it is highly probable that aggressive thresholds
 526 $q_{\pm}^{(1)}$ will be adequate to generate keys at a faster rate. If this
 527 condition is held for $INT_{SUCCESS}$ times, it is reasonable to
 528 consider these thresholds as neutral, assigning $q_{\pm}^{(2)} = q_{\pm}^{(1)}$
 529 and recalculating the others according to formulae 29 and 30. Sec-
 530 ondly, when the algorithm reaches the maximum and channel
 531 reciprocity is stable, it is more likely that neutral thresholds
 532 $q_{\pm}^{(2)}$ will be valid, leaving all parameters unchanged as in

TABLE I
SIMULATION PARAMETERS

Parameter	Value	Description
<i>DATASIZE</i>	50000	No. channel estimates
<i>RUNS</i>	120	No. test runs
<i>L</i>	20	No. multipaths components
$u_{A(B)max}$	30 m/s	Vehicles max speeds
u_{Smax}	30 m/s	Scatterers max speed
$\alpha_{A(B),l}$	$\sim U[-\pi, +\pi]$	Azimuth angles
$\beta_{A(B),l}$	$\sim U[0, 1]$	Elevation angles
$\alpha_{1,l}, \alpha_{2,l}$	$\sim U[-\pi, +\pi]$	Scatterers angles
f_c	6 GHz	Carrier frequency
w_{Wb}	2.958	Weibull scale
a_{Wb}	0.428	Weibull shape

533 the previous attempt, thus avoiding oscillations. Finally, if we
 534 assume that the algorithm is using a smaller region concerning
 535 the current channel condition, only defensive thresholds are
 536 probably valid or else none, suggesting a shift $q_{\pm}^{(2)} = q_{\pm}^{(3)}$
 537 after INT_{FAIL} occurrences.

538 V. SIMULATIONS

539 During our tests, every simulation included 50,000 channel
 540 estimates, repeated for 120 runs to stabilise the resulting
 541 statistics. Furthermore, the number of multipath components
 542 was $L = 20$ to recreate a pure diffuse Rayleigh environment,
 543 capable of modelling an urban scenario. Since estimates have
 544 to be collected from uncorrelated different coherence region of
 545 duration T_{coh} , we use a fixed maximum probing rate $F_p =$
 546 $1/T_{coh}$. Other relevant configuration settings are presented in
 547 table I.

548 In a first set of experiments we evaluated the performance
 549 of the new thresholding strategies. A standard two-level quan-
 550 tisation scheme [19] with CASCADE has been modified to
 551 analytically derive the thresholds using CDF and AFD-based
 552 formulae presented in section IV. Figures 7 and 8 show SBGR
 553 performances against censor size for different non-reciprocity
 554 configurations modelled by standard deviation σ_C . Results
 555 are shown in table II where both approaches outperform the
 556 standard one in all scenarios, especially with worse reciprocity.
 557 Performances are substantially equivalent, where CDF scores
 558 slightly better results in correspondence to $\sigma_C = 0.20$ and
 559 $\sigma_C = 0.30$, whilst AFD results superior in all other setups.
 560 The same table also illustrates how both analytical strategies
 561 are able to generate high entropy keys, even in low reciprocity
 562 environments ($\sigma_C = 0.30$), where STD fails to do so.

563 In the second set of experiments, correctness and perfor-
 564 mance of the Perturb-Observe algorithm have been evaluated
 565 through extensive simulation. As the baseline, we introduced
 566 a quantisation scheme, referred to as EX-SEARCH, where the
 567 thresholds are chosen directly from a lookup table. The latter
 568 has been created through exhaustive search, containing the
 569 optimal thresholds for various non-reciprocity settings in the
 570 range $\sigma_C \in [0.10, 0.30]$. Figure 9 shows PO algorithm's per-
 571 formance against EX-SEARCH. CDF and AFD configurations
 572 provide similar results, however, they both outperform EX-
 573 SEARCH, emphasising the superiority of our self-configurable

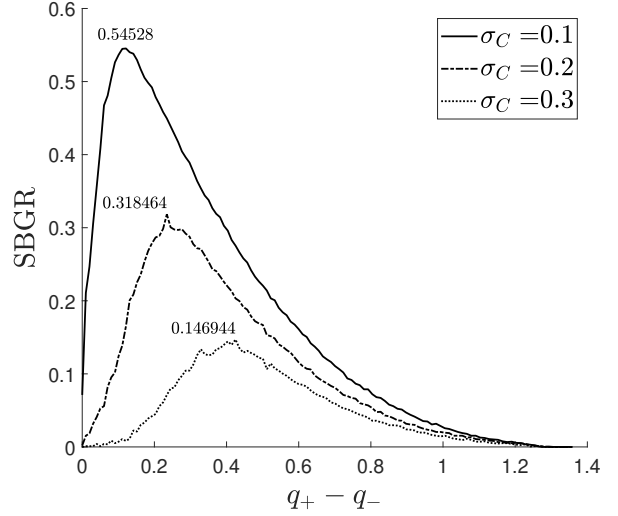


Fig. 7. CDF-thresholding strategy for different non-reciprocity factors.

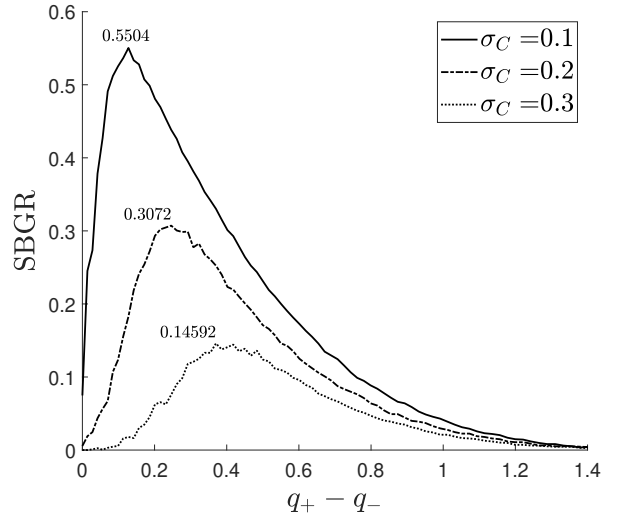


Fig. 8. AFD-thresholding strategy for different non-reciprocity factors.

574 approach. In fact, these better results are due to PO's ability
 575 to adapt and exploit the time intervals, where the random
 576 estimates temporally allow for a smaller censor size hence,
 577 a higher BGR.

578 In the last set of experiments, we applied NIST test suite
 579 [13] to the bit-streams generated by our algorithm in order
 580 to prove the absence of statistical defects. Each test returns
 581 a P-value indicating the strength of the evidence against the
 582 null hypothesis. More specifically, when the returned P-value
 583 is larger than the chosen significance level ($\alpha_{sig} = 0.01$),
 584 the sequence can be considered as random. Nonetheless, four
 585 tests, namely 'Binary Matrix Rank', 'Overlapping Template
 586 Matching', 'Maurers Universal' and 'Linear Complexity', re-
 587 quire an extremely long streams, which cannot be provided
 588 by this specific simulator and hence they were excluded.

TABLE II
RESULTING SBGR AND ENTROPY OF STD, CDF AND AFD APPROACHES

σ_C	STD		CDF		AFD	
	SBGR	H	SBGR	H	SBGR	H
0.10	0.5309	0.9935	0.5453 (+2.71%)	0.9947	0.5504 (+3.76%)	0.9941
0.15	0.4122	0.9933	0.4188 (+1.60%)	0.9937	0.4270 (+3.59%)	0.9941
0.20	0.2796	0.9934	0.3185 (+13.91%)	0.9940	0.3072 (+9.87%)	0.9932
0.25	0.1946	0.9934	0.2068 (+6.27%)	0.9939	0.2140 (+9.97%)	0.9925
0.30	0.1157	0.5252	0.1469 (+26.97%)	0.9942	0.1423 (+22.99%)	0.9920

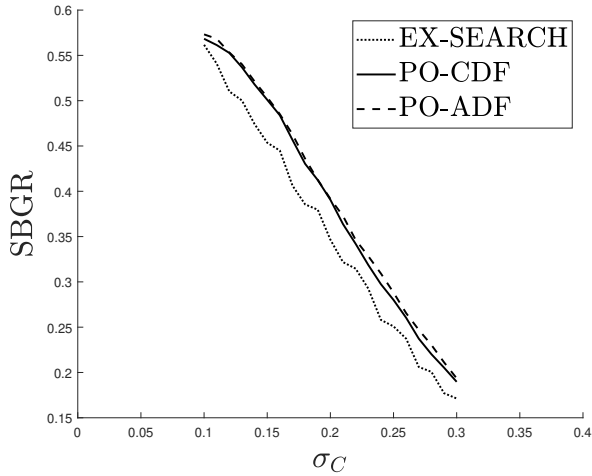


Fig. 9. Performance of Perturb-Observe algorithm compared to exhaustive search .

The results obtained proved that the new approaches can better exploit channel randomness and generate a higher number of keys than the existing standard scheme. More importantly, the PO algorithm is capable of adapting to varying reciprocity conditions, which makes it independent of empirical choices of parameters that often do not behave well in scenarios not previously tested. Robustness of the generated keys was tested evaluating their respective Shannon entropies as well as, against the NIST tests suite. In both cases, the resulting sequences are considered as random thus, being resilient to statistical attacks.

Further research is recommended in the application of the PO algorithm to various deterministic channel models for VANETS in more specific environments. Moreover, it is desirable to investigate other error correction schemes, besides CASCADE, in order to evaluate their positive or negative impacts on SBGR and investigate further the evolution of the proposed adaptive algorithm.

REFERENCES

- [1] L. Gafencu, L. Scripcariu, and I. Bogdan, "An overview of security aspects and solutions in vanets," in *2017 International Symposium on Signals, Circuits and Systems (ISSCS)*, 2017, pp. 1–4.
- [2] H. Hasrouny, A. E. Samhat, C. Bassil, and A. Laouiti, "Vanet security challenges and solutions: A survey," *Vehicle Communications*, vol. 7, pp. 7 – 20, 2017. [Online]. Available: <http://www.sciencedirect.com/science/article/pii/S2214209616301231>
- [3] Y. Zou, J. Zhu, X. Wang, and L. Hanzo, "A survey on wireless security: Technical challenges, recent advances, and future trends," *Proceedings of the IEEE*, vol. 104, no. 9, pp. 1727–1765, 2016.
- [4] A. J. Menezes, S. A. Vanstone, and P. C. V. Oorschot, *Handbook of Applied Cryptography*, 1st ed. USA: CRC Press, Inc., 1996.
- [5] E. C. Eze, S.-J. Zhang, E.-J. Liu, and J. C. Eze, "Advances in vehicular ad-hoc networks (VANETs): Challenges and road-map for future development," *International Journal of Automation and Computing*, vol. 13, no. 1, pp. 1–18, 2016.
- [6] D. E. Kouicem, A. Bouabdallah, and H. Lakhlef, "Internet of things security: A top-down survey," *Computer Networks*, vol. 141, pp. 199 – 221, 2018. [Online]. Available: <http://www.sciencedirect.com/science/article/pii/S1389128618301208>
- [7] M. Bloch, J. Barros, M. R. D. Rodrigues, and S. W. McLaughlin, "Wireless information-theoretic security," *IEEE Transactions on Information Theory*, vol. 54, no. 6, pp. 2515–2534, 2008.
- [8] A. Goldsmith, *Wireless Communications*. USA: Cambridge University Press, 2005.
- [9] M. Bottarelli, G. Epiphaniou, D. K. B. Ismail, P. Karadimas, and H. Al-Khateeb, "Physical characteristics of wireless communication channels for secret key establishment: A survey of the research," *Computers & Security*, vol. 78, pp. 454 – 476, 2018. [Online]. Available: <http://www.sciencedirect.com/science/article/pii/S0167404818300841>
- [10] G. S. Smith, "A direct derivation of a single-antenna reciprocity relation for the time domain," *IEEE Transactions on Antennas and Propagation*, vol. 52, no. 6, pp. 1568–1577, 2004.

Table III shows the P-values of the different tests for different reciprocity conditions. CDF has occasionally failed the 'random excursions' tests in case of low channel reciprocity, whilst AFD proved to be always successful. Despite this, both techniques clearly proved to be able to generate random sequences, which can be safely used as cryptographic keys.

VI. CONCLUSIONS

In this paper, we proposed a new analytical method for the generation of quantisation thresholds in the Physical Layer Security extraction process from the channel RSS values. In contrast to the standard level-crossing approach, the presented CDF and AFD techniques guarantee the optimality of the entropy of the resulting keys. Additionally, using these methods we introduced a quantisation optimisation engine as a feedback block in the key generation process. The proposed PO algorithm changes the size of the invalid region and observes the results to identify the maximum point of the SBGR metric, which in turn simultaneously captures both the bit generation rate and the bit mismatch rate. Although the techniques discussed apply to different wireless propagation environments, the use of VANETS in an urban environment has been chosen as the use-case in this work. We implemented a three-dimensional stochastic model of a V2V channel, including the interaction between mobile scatterers as well as, first and second-order statistics.

TABLE III
RESULTS OF NIST TESTS ON THE PO ALGORITHM WITH CDF AND AFD THRESHOLDING STRATEGIES

Test (128-bit keys)	PO-CDF			PO-AFD		
	$\sigma_C = 0.10$	$\sigma_C = 0.20$	$\sigma_C = 0.30$	$\sigma_C = 0.10$	$\sigma_C = 0.20$	$\sigma_C = 0.30$
monobit	0.7798	0.0736	0.0292	0.4338	0.8230	0.1312
frequency	0.7328	0.5190	0.0336	0.8197	0.9705	0.4008
runs	0.9982	0.9374	0.1211	0.8096	0.3412	0.8604
longest run ones	0.0610	0.6601	0.9287	0.4793	0.6442	0.7589
dft	0.3049	0.7975	0.3049	0.7975	0.4416	0.6079
non overlapping template matching	0.9996	0.9931	0.8218	0.9935	0.9373	0.5865
serial	0.4731	0.5528	0.0321	0.2649	0.5620	0.2867
approximate entropy	0.5468	0.5719	0.0326	0.6215	0.8187	0.2970
cumulative sums	0.8982	0.0471	0.0113	0.5492	0.7797	0.1075
random excursions	0.0158	0.0001	0.0018	0.0238	0.0957	0.0445
random excursions variant	0.0514	0.0005	0.1597	0.0593	0.0156	0.1991

- 666 [11] IEEE Computer Society, "IEEE Standard for Information technology–
667 Telecommunications and information exchange between systems Local
668 and metropolitan area networks–Specific requirements Part 11: Wireless
669 LAN Medium Access Control (MAC) and Physical Layer (PHY) Spec-
670 ifications," *IEEE Std 802.11-2012 (Revision of IEEE Std 802.11-2007)*,
671 pp. 1–2793, 2012.
- 672 [12] C. E. Shannon, "A mathematical theory of communication," *Bell
673 System Technical Journal*, vol. 27, no. 3, pp. 379–423, 1948. [On-
674 line]. Available: [https://onlinelibrary.wiley.com/doi/abs/10.1002/j.1538-
675 7305.1948.tb01338.x](https://onlinelibrary.wiley.com/doi/abs/10.1002/j.1538-7305.1948.tb01338.x)
- 676 [13] A. Rukhin, J. Sota, J. Nechvatal, M. Smid, E. Barker, S. Leigh,
677 M. Levenson, M. Vangel, D. Banks, A. Heckert, J. Dray, and S. Vo, "A
678 statistical test suite for random and pseudorandom number generators
679 for cryptographic applications."
- 680 [14] N. Patwari, J. Croft, S. Jana, and S. K. Kasera, "High-rate uncorrelated
681 bit extraction for shared secret key generation from channel measure-
682 ments," *IEEE Transactions on Mobile Computing*, vol. 9, no. 1, pp.
683 17–30, 2010.
- 684 [15] Hongbo Liu, Jie Yang, Yan Wang, and Yingying Chen, "Collaborative
685 secret key extraction leveraging received signal strength in mobile
686 wireless networks," in *2012 Proceedings IEEE INFOCOM*, 2012, pp.
687 927–935.
- 688 [16] J. Croft, N. Patwari, and S. K. Kasera, "Robust uncorrelated bit
689 extraction methodologies for wireless sensors," in *Proceedings of the
690 9th ACM/IEEE International Conference on Information Processing in
691 Sensor Networks*, ser. IPSN '10. New York, NY, USA: Association
692 for Computing Machinery, 2010, p. 70–81. [Online]. Available:
693 <https://doi.org/10.1145/1791212.1791222>
- 694 [17] G. Epiphaniou, P. Karadimas, D. Kbaier Ben Ismail, H. Al-Khateeb,
695 A. Dehghantanha, and K. R. Choo, "Nonreciprocity compensation
696 combined with turbo codes for secret key generation in vehicular ad
697 hoc social iot networks," *IEEE Internet of Things Journal*, vol. 5, no. 4,
698 pp. 2496–2505, 2018.
- 699 [18] S. Bakshi, J. Snoap, and D. C. Popescu, "Secret key generation using
700 one-bit quantized channel state information," in *2017 IEEE Wireless
701 Communications and Networking Conference (WCNC)*, 2017, pp. 1–6.
- 702 [19] S. Mathur, W. Trappe, N. Mandayam, C. Ye, and A. Reznik, "Securing
703 Wireless Communications at the Physical Layer," pp. 201–230, 2009.
- 704 [20] A. D. Wyner, "The Wire-Tap Channel," *Bell System Technical Journal*,
705 vol. 54, no. 8, pp. 1355–1387, oct 1975.
- 706 [21] U. Maurer, "Secret key agreement by public discussion from common
707 information," *IEEE Transactions on Information Theory*, vol. 39, no. 3,
708 pp. 733–742, may 1993.
- 709 [22] R. Ahlswede and I. Csiszar, "Common randomness in information theory
710 and cryptography. I. Secret sharing," *IEEE Transactions on Information
711 Theory*, vol. 39, no. 4, pp. 1121–1132, jul 1993.
- 712 [23] G. Brassard and L. Salvail, "Secret-Key Reconciliation by Public Dis-
713 cussion," in *Advances in Cryptology — EUROCRYPT '93*. Berlin,
714 Heidelberg: Springer Berlin Heidelberg, 1994, pp. 410–423.
- 715 [24] S. Bakshi, J. Snoap, and D. C. Popescu, "Secret Key Generation Using
716 One-Bit Quantized Channel State Information," in *2017 IEEE Wireless
717 Communications and Networking Conference (WCNC)*. IEEE, mar
718 2017, pp. 1–6.
- 719 [25] R. Impagliazzo, L. A. Levin, and M. Luby, "Pseudo-random Generation
720 from One-way Functions," in *Proceedings of the Twenty-first Annual
ACM Symposium on Theory of Computing*, ser. STOC '89. New York,
721 NY, USA: ACM, 1989, pp. 12–24. [Online]. Available:
722 <http://doi.acm.org/10.1145/73007.73009>
- 723 [26] Y. E. H. Shehadeh and D. Hogrefe, "A survey on secret key generation
724 mechanisms on the physical layer in wireless networks," *Sec. and
725 Commun. Netw.*, vol. 8, no. 2, p. 332–341, Jan. 2015. [Online].
726 Available: <https://doi.org/10.1002/sec.973>
- 727 [27] M. Tope and J. McEachen, "Unconditionally secure communications
728 over fading channels," in *2001 MILCOM Proceedings Communications
729 for Network-Centric Operations: Creating the Information Force (Cat.
730 No.01CH37277)*, vol. 1. IEEE, 2001, pp. 54–58.
- 731 [28] B. Azimi-Sadjadi, A. Kiayias, A. Mercado, and B. Yener, "Robust key
732 generation from signal envelopes in wireless networks," in *Proceedings
733 of the 14th ACM conference on Computer and communications security
734 - CCS '07*. New York, New York, USA: ACM Press, 2007, p. 401.
- 735 [29] M. Yuliana, Wirawan, and Suwadi, "Performance evaluation of the key
736 extraction schemes in wireless indoor environment," in *2017 Interna-
737 tional Conference on Signals and Systems (ICSigSys)*. IEEE, may 2017,
738 pp. 138–144.
- 739 [30] S. Jana, S. N. Premnath, M. Clark, S. K. Kasera, N. Patwari, and
740 S. V. Krishnamurthy, "On the effectiveness of secret key extraction from
741 wireless signal strength in real environments," in *Proceedings of the 15th
742 annual international conference on Mobile computing and networking -
743 MobiCom '09*. New York, New York, USA: ACM Press, 2009, p. 321.
- 744 [31] B. Zan, M. Gruteser, and F. Hu, "Key Agreement Algorithms for
745 Vehicular Communication Networks Based on Reciprocity and Diversity
746 Theorems," *IEEE Transactions on Vehicular Technology*, vol. 62, no. 8,
747 pp. 4020–4027, 2013.
- 748 [32] X. Li, J. Liu, Q. Yao, and J. Ma, "Efficient and Consistent Key Extraction
749 Based on Received Signal Strength for Vehicular Ad Hoc Networks,"
750 *IEEE Access*, vol. 5, pp. 5281–5291, 2017.
- 751 [33] J. Wan, A. Lopez, and M. A. A. Faruque, "Physical Layer Key Genera-
752 tion: Securing Wireless Communication in Automotive Cyber-Physical
753 Systems," *ACM Transactions on Cyber-Physical Systems*, vol. 3, no. 2,
754 pp. 1–26, 2018.
- 755 [34] X. Zhu, F. Xu, E. Novak, C. C. Tan, Q. Li, and G. Chen, "Extracting
756 Secret Key from Wireless Link Dynamics in Vehicular Environments,"
757 *2013 Proceedings IEEE INFOCOM*, pp. 2283–2291, 2013.
- 758 [35] J. Maurer, T. Fugen, T. Schafer, and W. Wiesbeck, "A new inter-
759 vehicle communications (ivc) channel model," in *IEEE 60th Vehicular
760 Technology Conference, 2004. VTC2004-Fall. 2004*, vol. 1, 2004, pp.
761 9–13 Vol. 1.
- 762 [36] G. Matz and F. Hlawatsch, "Chapter 1 - fundamentals of
763 time-varying communication channels," in *Wireless Communications
764 Over Rapidly Time-Varying Channels*, F. Hlawatsch and G. Matz,
765 Eds. Oxford: Academic Press, 2011, pp. 1 – 63. [Online]. Available:
766 <http://www.sciencedirect.com/science/article/pii/B9780123744838000017>
- 767 [37] P. Karadimas and D. Matolak, "Generic stochastic modeling of
768 vehicle-to-vehicle wireless channels," *Vehicular Communications*,
769 vol. 1, no. 4, pp. 153–167, 2014. [Online]. Available:
770 <http://dx.doi.org/10.1016/j.vehcom.2014.08.001>
- 771 [38] P. Hirschhausen, L. M. Davis, D. Haley, K. Lever, L. Davis, D. Haley,
772 and K. Lever, "Identifying Key Design Parameters for Monte Carlo
773 Simulation of Doppler Spread Channels," pp. 33–38, 2014.
- 774

- 775 [39] P. Hoeher, "A Statistical Discrete-Time Model for the WSSUS Multipath
776 Channel," *IEEE Transactions on Vehicular Technology*, vol. 41, no. 4,
777 pp. 461–468, 1992.
- 778 [40] Q. Wang, H. Su, K. Ren, and K. Kim, "Fast and scalable secret key
779 generation exploiting channel phase randomness in wireless networks,"
780 *2011 Proceedings IEEE INFOCOM*, pp. 1422–1430, 2011.
- 781 [41] T. Wang, Y. Liu, and A. V. Vasilakos, "Survey on channel reciprocity
782 based key establishment techniques for wireless systems," *Wirel.*
783 *Netw.*, vol. 21, no. 6, p. 1835–1846, Aug. 2015. [Online]. Available:
784 <https://doi.org/10.1007/s11276-014-0841-8>